Article

pubs.acs.org/Biomac

Heparin Decamer Bridges a Growth Factor and an Oligolysine by Different Charge-Driven Interactions

Burcu Baykal Minsky,[†] Thuy V. Nguyen,[‡] Shelly R. Peyton,[‡] Igor A. Kaltashov,[†] and Paul L. Dubin*[,†]

Departments of [†]Chemistry and [‡]Chemical Engineering, University of Massachusetts, 710 North Pleasant Street, Amherst, Massachusetts 01003, United States

Supporting Information

ABSTRACT: Full-length heparin is widely used in tissue engineering applications due its multiple protein-binding sites that allow it to retain growth factor affinity while associating with oligopeptide components of the tissue scaffold. However, the extent to which oligopeptide coupling interferes with cognate protein binding is difficult to predict. To investigate such simultaneous interactions, we examined a well-defined ternary system comprised of acidic fibroblast growth factor (FGF), tetralysine (K_4), with a heparin decamer (dp10) acting as a noncovalent coupler. Electrospray ionization mass spectrometry was used to assess binding affinities and complex stoichiometries as a function of ionic strength for dp10·K_4 and FGF·dp10. The ionic strength dependence of K_4·dp10 formation is qualitatively consistent with binding driven by the release of condensed counterions previously suggested for native heparin with divalent oligopeptides (Mascotti, D. P.; Lohman, T. M. *Biochemistry* 1995, *34*, 2908−2915). On the other hand, FGF binding displays more complex ionic strength dependence, with higher salt resistance. Remarkably, dp10 that can bind two FGF molecules can only bind one tetralysine. The limited binding of K_4 to dp10 suggests that the tetralysine might not block growth factor binding, and the 1:1:1 ternary complex is indeed observed. The analysis of mass distribution of the bound dp10 chains in FGF·dp10, FGF_2·dp10, and FGF·dp10·K_4 complexes indicated that higher degrees of dp10 sulfation promote the formation of FGF_2·dp10 and FGF·dp10·K_4. Thus, the selectivity of appropriately chosen short heparin chains could be used to modulate growth factor sequestration and release in a way not feasible with heterogeneous native heparin. In support of this, human hepatocellular carcinoma cells (HEP3Bs) treated with FGF·dp10·K_4 were found to exhibit biological activity similar to cells treated with FGF.

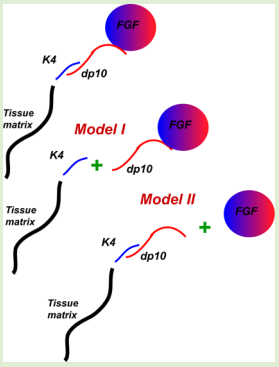

INTRODUCTION

Glycosaminoglycans (GAGs) such as heparin (Hp) are incorporated into tissue engineering scaffolds with the intention of mimicking their ability in the extracellular matrix (ECM) to sequester and release numerous growth factors (GFs).[1−4] Effective assembly strategies accomplish this through specific and nonspecific association of GAGs with matrix components such as peptides. Model ternary systems can facilitate in vitro investigation of simultaneous complex formation among glycosaminoglycans, growth factors, and scaffold elements, revealing how noncovalent, for example, electrostatic, interactions can be utilized. Combination of growth factors with peptide and GAG components *of reduced heterogeneity* is currently necessary in order to analyze these ternary systems with powerful characterization techniques such as electrospray ionization mass spectrometry (ESI-MS).

GF-binding heparinoids have been coupled to scaffold polymers in order to achieve modulated release of the protein either with or without heparin. The covalent attachment of heparin to scaffolds has been pursued through many strategies,[5−12] which may obstruct GF binding sites or introduce toxic cross-linking agents.[13] This is avoided by means of oligopeptide scaffold components that bind heparin noncovalently.[11,13−16] The scaffold structure and Hp-oligopeptide affinity determine the release rate of Hp-GF.[13,14] The strength of the heparin-GF bond determines both the rate of GF release and whether it is released along with bound Hp. It is therefore important to consider whether differences in the nature of two interactions allow them to be independently modulated by either ionic strength or heparin microstructure.

The model used here for the binding of oliogpeptides to heparin originates from the counterion condensation theory of Manning,[17,18] initially developed to describe the binding of oligolysines to DNA.[19,20] In the oligolysine-DNA case, the driving force is the entropy of the release of DNA counterions (Na^+) from the condensed layer. This leads to a particular form of the ionic strength dependence of the binding constant: $-\log K_{obs} \sim n \log I$, where K_{obs} is the equilibrium association constant, I is ionic strength, and n is ligand charge. Lohman and Mascotti[21] applied this concept to oligopeptide/heparin binding (conceptually replacing DNA with heparin) and measured the salt dependence of the binding constants. Finding linearity of log K_{obs} versus log I for heparin and cationic oligopeptides, they concluded that the measured ΔG_{obs} was purely entropic. This observation, along with recent direct measurement of counterion condensation by heparin,[22]

Received: August 14, 2013
Revised: October 8, 2013
Published: October 9, 2013

provides strong evidence for the release of condensed counterion during the binding of cationic ligands to heparin. However, further extension of the Manning-Record model in which the oligopeptide has been replaced by a protein[23−25] has since been questioned on the basis of fundamental uncertainty regarding the expanded role of long-range interactions.[26]

While noncovalent coupling of growth factors to Hp is recognized as a valuable approach for the development of biofunctional tissue surrogates, questions arise about "electrostatic" heparin-oligolysine binding versus "specific" Hp−GF interactions. The former has been widely accepted as nonspecific, but the precise nature of the latter has remained controversial. Models based on the definition of Hp-GF as a cognate system emphasize "specific", that is, short-range forces comprising hydrophobic and pairwise interactions (H-bonding and salt bridges).[27−30] These are thought to impose on heparin precise structural and conformational requirements for protein recognition. However, there is increasing evidence that strong binding occurs between globally negative heparin-binding proteins and polyanions,[31] especially when polyanion charge distributions are arranged in a way that minimizes long-range repulsion, while optimizing short-range attractions with locally positive protein domains.[32−34] This can result in a level of selectivity that does not arise from short-range interactions such as hydrogen-bonding or "ion-pair" formation.[31,35] Supporting this perspective, recent findings indicate that various FGFs share the same GF-binding sites on HS,[36,37] where binding affinity is correlated with the extent of sulfation.[37] Catlow et al. showed that the interaction of hepatocyte growth factor/scatter factor with HS is dominated by electrostatics inasmuch as sulfate density, as opposed to the presence of particular types of sulfation, affects the selectivity.[38] Thus, the interactions considered here could be intrinsically promiscuous[39,40] and dominated by columbic forces. There is also growing evidence that these interactions can be highly selective.[41,42]

When Hp−GF interactions are viewed in the context of the vast array of polyelectrolyte−protein interactions,[43] the role of ionic strength is to diminish long-range electrostatic interactions between Hp and complementary protein positive "patches,"[43] an effect typically parametrized by the Debye−Hückel screening length κ^{-1}.[34,35,44,45] The possible role of long-range interactions also leads directly to consideration of long-range repulsion between Hp and the negatively charged domains of many of its morophogen cognates,[46] an additional issue when the oligocationic "ligand" in the Record-Manning model is envisioned as part of a protein that may be larger than its heparinoid "host".

The differences in the effects of both Hp microstructure and ionic strength on the two types of interactions could make it possible to control the relative strengths of Hp−GF and Hp−oligopeptide interactions either by using appropriate heparin fractions or by adjusting salt concentration. Hp microstructure, difficult to define for the immensely heterogeneous native heparin, can be better identified using GF-specific oligoheparins. The length of such oligoheparins must be sufficient to allow for noncovalent binding to both scaffold oligopeptide units and growth factors. Competition between oligopeptide and GF for the heparin chains could then be modulated if the two types of binding are driven by different mechanisms, for example, counterion release for the former and the screened electrostatics for the latter. These differences could make it possible to tune the two interactions so that binding of oligopeptide and GF could take place simultaneously. In theory, end effects on counterion condensation by heparin oligomers[47] suggest that the central saccharide units, rich in condensed counterions,[22] could provide unique sites for Record-Manning type oligolysine binding, leaving the distal heparin units available for screened GF binding, that is, suppressed at length scales larger than the Debye length, κ^{-1} (nm) $\approx 0.3I^{-1/2}$ in 1:1 electrolyte.

The model system studied in this work allows for in vitro investigation of simultaneous complex formation among low MW GAGs, GFs, and scaffold peptide elements. The mechanism of ternary and binary complex formation involving these species could contribute to molecular level understanding of the assembly of scaffolds and their ultimate behavior in cell culture. A specific hypothesis to be tested is that the GF binding sites within a given chain have unique sulfate charge densities. Elucidation of protein "recognition sites" on heparin has been pursued by crystallography, typically involving assumptions about certain pairwise interactions not directly related to sulfate charge densities.[48,49]

In this work, ESI-MS is applied to determine the stoichiometry and ionic strength dependences for a ternary model system comprising FGF-1, a heparin decamer (dp10) and tetralysine (K_4). ESI-MS of native state proteins has recently evolved as a very important tool to detect their noncovalent complexes, revealing compositional details of the ligand-protein complexes.[50−52] Increased sensitivity, low sample requirements, and applicability to transient complexes have improved the importance of native ESI-MS. We examined the effects of ionic strength on the FGF-1·dp10 and K4·dp10 interactions, and found the latter but not the former to be analogous to the well-known oligolysine-oligonucleotide electrostatic model.[19,26] Furthermore, our results indicated that the ability of the components of dp10 to engage in the ternary complex or bind multiple growth factors depends on their sulfation levels.

EXPERIMENTAL SECTION

Materials. Heparin decasaccharide (dp10), prepared by high-resolution gel filtration of partial heparin lyase digestion of high quality heparin, was generously donated by Prof. John Gallagher from Iduron (Manchester, U.K.). Acidic fibroblast growth factor (includes His to Gly 93 mutation to increase stability,[53] pI = 7.8) was provided by Prof. Robert Linhardt (RPI, Troy, NY). Tetralysine (K_4) was purchased from Sigma.

Methods. *Mass Spectrometry.* All experiments were performed with a QStar-XL hybrid quadrupole-time-of-flight MS equipped with a nano-ESI source (AB Sciex, Toronto, Canada). The measurements were performed using closed (2 μm id) glass nanospray capillaries (New Objective, Woburn, MA). FGF·dp10 binding experiments were acquired using following settings of ion optics in the ESI interface: DP, 100; FP, 265; DP2, 15. K_4 and dp10 binding experiments were performed utilizing mild ion desolvation conditions (DP, 40; FP, 150; DP2, 15). FGF-1 was buffer exchanged using Amicon (10 kDa cut off) with 100 mM $NH_4CH_3CO_2$, and the protein concentration was verified by UV−vis using molar absorptivity of 17545 M^{-1} cm^{-1}. FGF, dp10, and K_4 were diluted from the stock solutions to the final concentrations (2, 3, and 10 μM, respectively) in the desired ammonium acetate concentrations. ESI-MS was used to determine stoichiometries of FGF-1·dp10 complexes, and m/z values of the protein and the complexes were assigned with BioAnalyst v1.1.5 (MDS Sciex/Applied Biosystems, Toronto, Canada). The mass distribution of the protein-bound heparinoid molecules were calculated using the following formula:

$$((m/z)\cdot z - z) - n\cdot M_{\mathrm{FGF}} \quad (1)$$

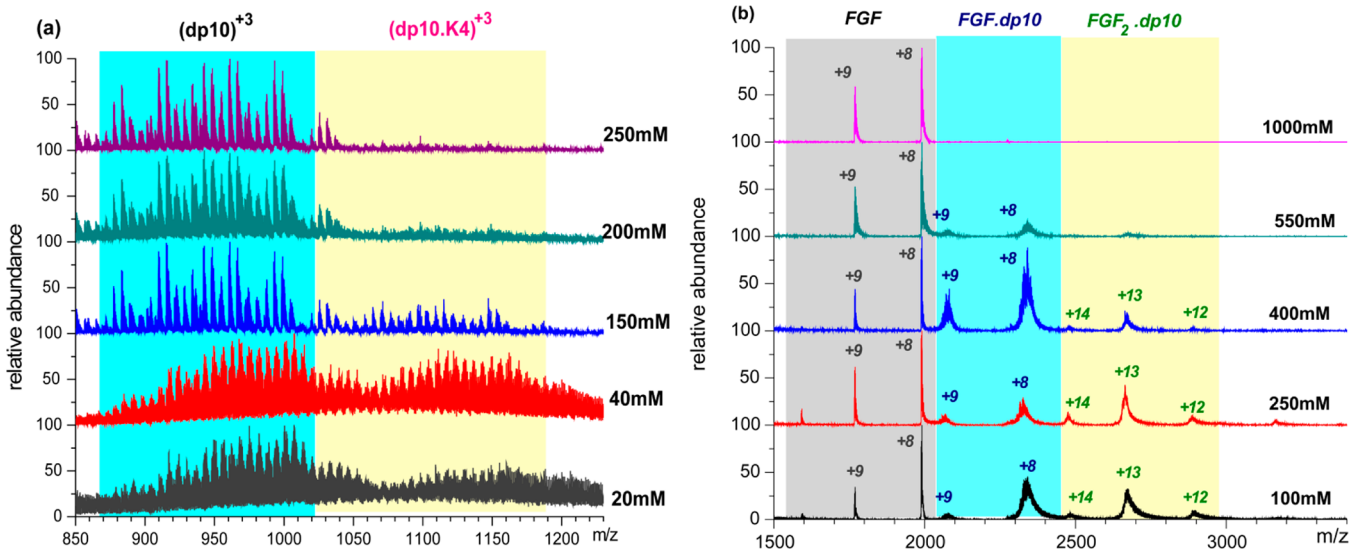

Figure 1. (a) ESI mass spectra of dp10 (3 μM) and K_4 (10 μM) in pH 6.8 ammonium acetate at varying ionic strengths. Not shown: free K_4 (m/z = 531, z = +1). (b) ESI mass spectra of FGF-1 (2 μM) and dp10 (3 μM) in 100, 250, 400, 550, and 1000 mM ammonium acetate. The shaded columns represent (a) dp10 and dp10·K_4; (b) FGF, FGF·dp10, and FGF_2·dp10.

where n represents total number bound FGF-1 molecules and M_{FGF} is the mass of a single FGF molecule. Because all analyses were performed in the positive ion mode, it is expected that each ionic species will also contain 4−5 cations (Na^+ or NH_4^+).[50] Shaded boxes are used in Figures 3 and 5 to indicate the mass ranges for heparinoid species with different extent of sulfation (the overlap is due to the uncertainty in the number of cationizing agents attached to each polyanionic chain).

Computational. DelPhi V. 4r1.1,[54,55] which applies nonlinear Poisson−Boltzmann equation to generate the potential surface of the protein, was used to model the electrostatic potential around FGF-1 (PDB id: 1K5U) and heparin decamer (solution NMR: 1HPN). The structures were taken from the protein data bank (http://www.rcsb.org/). The charges of amino acids on the protein were determined using the spherical-smeared charged model put forward by Tanford.[56]

Cell Culture and Proliferation Assays. All cell culture supplies were purchased from Life Technologies, Carlsbad, CA, unless otherwise noted. Human hepatocellular carcinoma cells (HEP3Bs, American Type Culture Collection, Manassas, VA) were cultured in modified Eagle's medium (MEM) supplemented with 10% Fetal Bovine Serum (FBS) and 1% penicillin-streptomycin (P/S) at 37 °C and 5% CO_2. To quantify cell growth in response to growth factors and growth factor complexes, HEP3Bs were seeded at 10000 cells/well in 96-well plates (Corning, Tewksbury, MA) in standard growth medium. After 24 h, the medium was replaced with the serum-free medium containing 1% P/S and either fibroblast growth factor (FGF) or FGF·dp10.K4, ranging from 0 to 50 ng/mL. We used the CellTiter 96 AQueous One Solution Cell Proliferation Assay (Promega, Madison, WI) to measure cell proliferation at 24 and 72 h. After 3 h of incubation, the absorbance was read at 490 nm with a BioTek ELx800 microplate reader (BioTek, Winooski, VT).

Statistical Analysis. One-way ANOVAs were performed with using Prism v5.04 (GraphPad Software, La Jolla, CA), the Tukey post-test was used to determine significance of pairwise differences. Data are reported as mean ± standard error with N = 3. $P \leq 0.05$ is denoted with *, ≤0.01 with **, and ≤0.001 with ***.

RESULTS AND DISCUSSION

1. K_4 Binding to dp 10. Figure 1 shows the effect of ionic strength on the binding of dp10 at pH 6.8 to K_4 (a) and to FGF (b). Even though K_4 is in molar excess (10:3 K_4/dp10), K_4 forms only a 1:1 complex with dp10. This is in contrast to the ability of dp10 to bind *at least* two FGF molecules. Furthermore, the contour length of dp10 (5 nm) is significantly larger than that of K_4 (~ 2 nm). It appears that the binding energy for the second K_4 is diminished, that is, binding is apparently anticooperative. Arguments based on variations in local sulfation would not explain why there are *no* dp10 chains that bind two oligolysines. We therefore explore the earlier studies of oligolysines and heparin, which supported the model put forward by Manning and Record.[57] As noted above, these studies showed that the driving force for oligocation binding to polyanion (e.g., DNA) is the entropy of the release of the polyanion's counterions from its condensed layer. A more recent theoretical result by Manning for oligo-polyelectrolytes is the diminution of condensation at and near chain ends,[47] subsequently verified by Minsky et al. for heparin oligomers.[22] Representation of the heparin disaccharide structure (Scheme 1, above) neglecting positional variations of sulfation leads to visualization of the chain as treated in the condensation model

Scheme 1. Representations of the Repeating Disaccharide Structure of Heparin (Reprinted with Permission from Ref 22. Copyright 2013 American Chemical Society)[a]

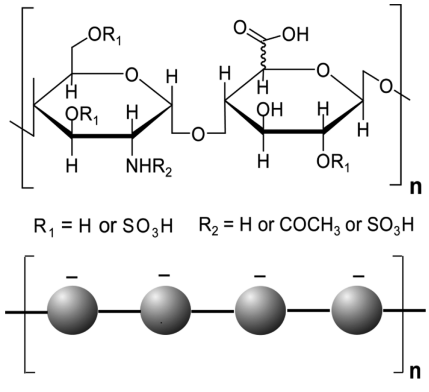

[a]Top: chemical structure shown with R1 and R2 groups. Bottom: representation of the disaccharide with the charge segments. The disaccharide is assumed to have four charges (three sulfates and one carboxylate, viewed identically).

dx.doi.org/10.1021/bm401227p | Biomacromolecules 2013, 14, 4091−4098

(Scheme 1, below), with the condensed counterion layer depleted at chain ends. If those ions are involved in the oligolysine binding process, the strongest K_4 binding site would comprise chain units far from the ends of dp10, that is, saccharides 3−8 (contour length ∼ 3 nm). The remaining distal regions are incompetent binders with respect to both length (1 nm) and condensed counterions. To further examine the applicability of this model, we examine whether the strong binding suppression with an increase from 40 to 150 mM ionic strength in Figure 1a is consistent with the condensed counterion model.

To compare dp10·K_4 results to those in the highly influential Mascotti and Lohmann paper,[20,21] it was necessary to extrapolate from the binding constants, K_{obs}, which were obtained in refs 20 and 21 for native heparin with a +2 oligolysine (n = 2). While their study[21] only covered a narrow range 12 < I < 30 mM, they obtained $K_{obs} \sim I^{-2}$, in agreement with theory in which the number of released counterions is equal to the ligand charge ($-(d \log K_{obs}/d \log I) = n$),[57] subsequently supported by Manning et al.[26] With n = 4, K_{obs} is expected to exhibit I^{-4} dependence for K_4. Thus, the dramatic suppression of binding seen in Figure 1a for the about 4-fold increase in I from 40 to 150 mM is entirely consistent with the 200-fold ((ca. 40/150)$^{-4}$) decrease in K_{obs}, as predicted by theory, suggesting that the binding of K_4 to dp10 is driven by the release of condensed counterions. The remarkably different I dependence in Figure 1b shows that a different mechanism must drive the binding of FGF to dp10 at 400 mM; binding based on the displacement of condensed counterions is not possible when the bulk ionic strength exceeds 380 mM, the local concentration of condensed counterions for heparin.[26]

2. FGF Binding to dp10. To compare binding strengths for FGF·dp10 versus K_4·dp10, the former was also investigated using salt concentration as a surrogate for binding affinity. Figure 1b shows the formation, in pH 6.8 ammonium acetate, of 1:1 and 2:1 complexes of FGF·dp10 at I = 100, 250, and 400 mM. If we use the salt resistance of complex formation as a measure of binding affinity, we find that the FGF·dp10 1:1 complex is more stable than the K_4·dp10 complex (see Figure 1), and also the FGF·dp10 2:1 complex. However, even the FGF·dp10 1:1 complex is fully suppressed at I > 550 mM, indicating the role of screened electrostatics. Although the pH used is only moderately lower that the pI, the charge distribution is anisotropic leading to a discernible positive domain (Figure 2).

Calculations of screened electrostatics by DelPhi have been recognized as a quantitative tool for elucidating the electrostatic binding energy of both protein−polyelectrolyte[58] and protein−protein interactions,[59] and comparisons with experimental results are facilitated by the display of electrostatic potential contours. The potential contours represented as grids in the DelPhi images arise from the conjoint sum of all possible pairwise coulomb forces that are subjected to the moderating influence of the ionic strength. This screening results from the asymmetric distribution of small ions, as parametrized by the Debye screening length ($\kappa^{-1} \sim I^{-1/2}$), the distance at which the electrical potential due to the protein surface charges decays to $1/e$ of the protein's surface potential. This approach, which needs to be clearly differentiated from the behavior of condensed counterions, explains the maximum in binding when $\kappa^{-1} \approx$ protein radius seen for binding at pH > pI for polyanions,[34] including heparin.[44]

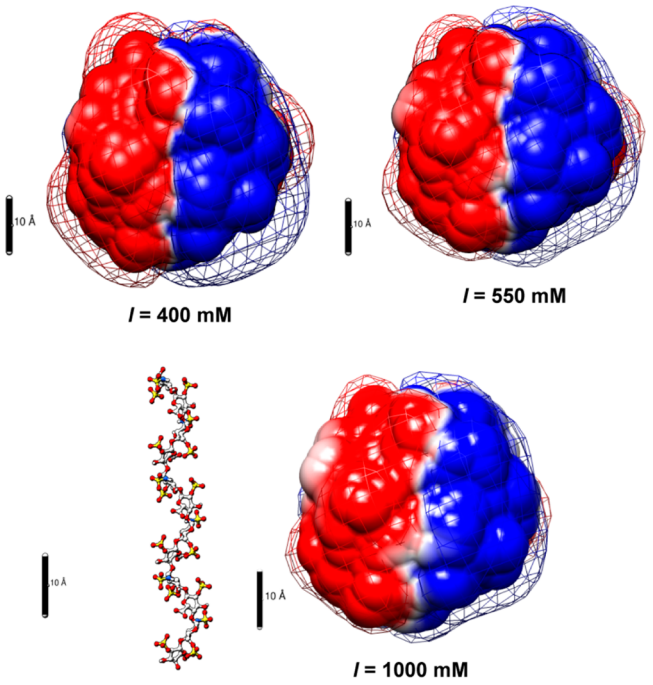

Figure 2. FGF-1 (PDB id: 1K5U) electrostatic images for pH 7.0 and I = 400, 550, and 1000 mM. The 5 Å surfaces (magnitude of charge shown by color intensity, blue positive, red negative) and equipotential surfaces (grids) +0.2 kT/e and −0.2 kT/e. The heparin decamer (solution NMR ID: 1HPN) is drawn to scale to help visualize its ability to reside within the FGF positive domain (sulfate groups are shown in yellow). The pH differences between Figure 1b and the DelPhi calculations have no significant effect on the amino acid charges.

This approach is reflected in the DelPhi images of Figure 2 for FGF at pH 7.0 and 400−1000 mM salt. The protein itself is represented at 5 Å from van der Waals surface to account for retention of heparin and FGF solvation, and the potential contour grids are presented at $\psi = 0.2kT/e$. As shown in Figure 2 for I = 400 mM, the volume between the 5 Å surface and the contour grid is sufficient to accommodate at least −5 heparin charges (1.5−2 disaccharide units, ∼2−3 nm dp10 segments), a dimension consistent with the FGF-binding site size on heparin.[60] The consequent electrostatic binding energy then is on the order of $1kT$, which represents the onset of binding.[58] The diminution of this volume seen with increasing salt portrays screening; therefore, the number of dp10 charges bound is reduced at 550 mM and abolished at 1000 mM, as seen in Figure 1b. The predominant role of screened electrostatics does not necessarily negate release of some bound counterions, but the number of these is debatable.[26]

The stability of the ternary complex requires not only that K_4 not compete with FGF, but also that the stronger binding of FGF to dp10 does not lead to its occupying all potential K_4-binding sites on dp 10. As noted in Figure 1, dp10 can bind either one or two FGF molecules; the ratio of FGF_2·dp10 to FGF·dp10 decreases with salt concentration I, most notably near I = 400 mM. This corresponds to a Debye length (κ^{-1} = 0.4 nm), suggesting that screening repulsions at that length scale could weaken the binding. To further explore the difference between the first and the second binding events, we consider the sulfation of the dp10 molecule found in FGF_2·dp10 versus those found in FGF·dp10. Figure 3 shows, in the absence of K_4, the mass spectra of FGF·dp10 complexes plotted

dx.doi.org/10.1021/bm401227p | Biomacromolecules 2013, 14, 4091−4098

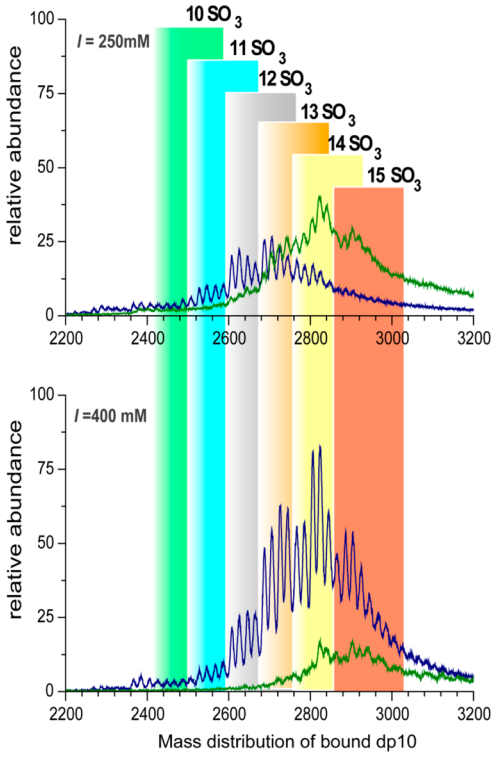

Figure 3. Mass distribution of protein-bound dp10 molecules in FGF·dp10 (blue trace) and FGF_2·dp10 (green trace) determined at ionic strengths of 250 and 400 mM.

on the adjusted mass scale where the mass of the protein component was subtracted from 2:1 and 1:1 complexes at 250 and 400 mM. Figure 3 represents in blue and green the collection of dp10 molecules found, respectively, in FGF·dp10 and in FGF_2·dp10. Given the presence of free FGF at all conditions, it might appear if one were to neglect the different sulfation patterns that the binding of FGF is anticooperative at high salt. A more reasonable explanation can be sought in differences in dp10 sulfation for the first and second binding sites, presumably higher for the high-affinity first site. The phase transition-like behavior of polyelectrolytes adsorption on oppositely charged surfaces can be extended to binding to oppositely charged colloids[61,62] and oppositely charged proteins.[63] Critical conditions for binding are then expressed by eq 2,

$$\sigma_c \, \xi \sim \kappa^b \tag{2}$$

where σ_c is the effective charge density of the protein positive patch, ξ is the polyelectrolyte structural linear charge density, b is an empirical scaling parameter, and κ (nm) $\approx 0.3I^{-1/2}$. According to eq 2, the critical ionic strength (above which no binding occurs) is described by $\kappa_c \sim \xi^{1/b}$. If the high-affinity first binding site is more highly sulfated, that is, $\xi^{I} > \xi^{II}$, then $\kappa_c^{I} > \kappa_c^{II}$, so binding at site I may persist when binding to site II is suppressed. Focusing on the results for the 1:1 complexes alone (blue trace in Figure 3), the increase in dp10 sulfation with ionic strength is consistent with eq 2. Typical values of b range from 0.5 to 3, a much smaller ionic strength dependence than the I^{-4} dependence of condensed counterion release, as noted in the comparison of Figure 1a,b.

3. Ternary Complex Formation. Figure 4a,b shows the ESI mass spectra of FGF, dp10, and K_4 of 2:3:10 (μM) stoichiometry at 20 and 100 mM ionic strengths, respectively. The signal from dp10·K_4 is not shown in Figure 4(a) due to excess noise, but K_4 does appear in the 1:1:1 FGF·dp10·K_4 (ternary) complex. The 5:1 excess of K_4 does not impede FGF binding, either because K_4 occupies an oligoheparin site distinct from that of FGF or because dp10·K_4 binding is intrinsically weaker. The ternary complex is less abundant at 100 mM (Figure 4b) most likely because high salt weakens the dp10·K_4 interaction (vide supra).

FGF·dp10 and FGF_2·dp10 complexes are observed, the former more abundant than the latter. The restriction of K_4 binding to one per chain, despite its small size, can be explained

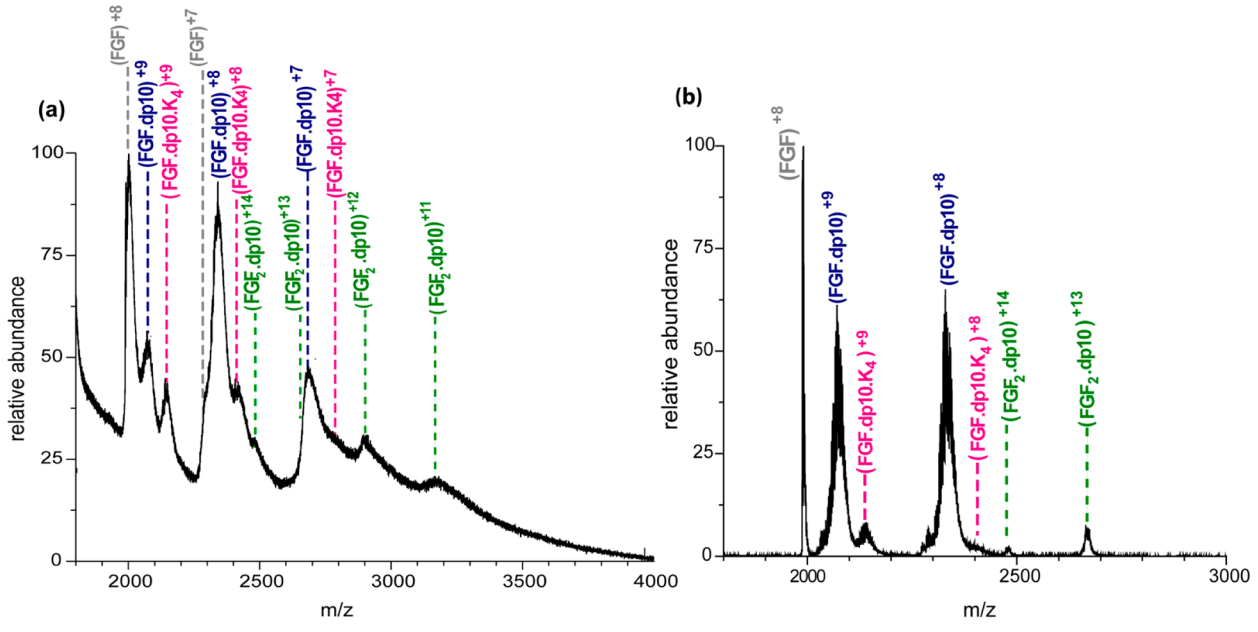

Figure 4. ESI mass spectra of a mixtures of FGF (2 μM), dp10 (3 μM), K_4 (10 μM) in 20 mM pH 6.8 (a) and 100 mM pH 5.5 (b). FGF present as FGF·dp10·K4; FGF·dp10; FGF_2·dp10; and free FGF.

dx.doi.org/10.1021/bm401227p | Biomacromolecules 2013, 14, 4091−4098

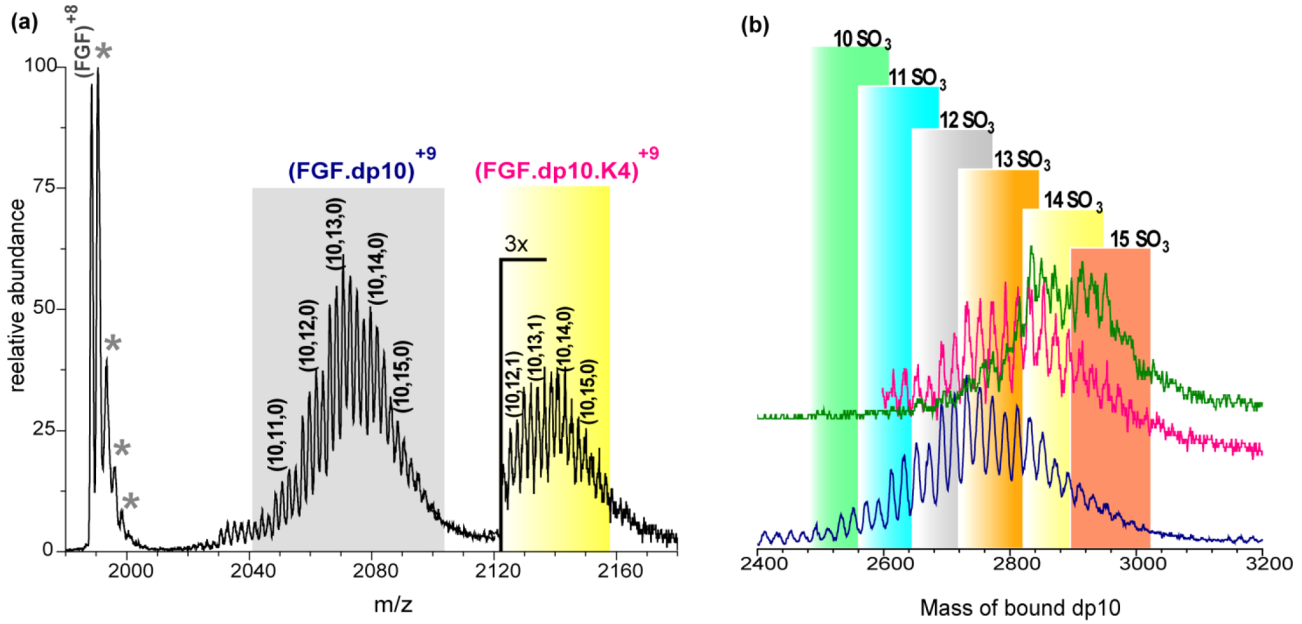

Figure 5. Assignment of sulfation levels of dp10 for the FGF·dp10·K4, FGF·dp10 and FGF_2·dp10 complexes presented in Figure 4b. (a) Expansion of the *m*/*z* regions of FGF·dp10.K4 and FGF·dp10 complexes (nomenclature by Roepstorff and Henriksen[64] for bound dp 10). NH_4^+ adducts on the unbound FGF are shown with asterisks (*). The *m*/*z* region of FGF·dp10·K4 is amplified 3 times for clarity. (b) Mass distribution of bound dp10 in FGF·dp10 (blue trace), FGF·dp10·K_4 (pink trace), and FGF_2·dp10 (green trace).

on the basis of the release of condensed counterions (vide supra), which are more abundant in the middle of dp10. On the contrary, if FGF binding were governed by screened electrostatics, the larger *effective* charge due to less counterion condensation at these terminal saccharides could account for facile binding of two FGF molecules per chain.

Expansion of the spectral region that comprises FGF·dp10 and ternary complex shown in Figure 4 reveal the levels of sulfation of the bound dp10 chains (Figure 5a,b). The sulfation density in the ternary complex, slightly higher than that seen in FGF·dp10, suggesting that dp10 chains with low sulfation (<S12) only bind to a single FGF, while those with higher sulfation (>S12) can bind K_4 along with FGF. The strong suppression of K_4 binding at high salt noted above is responsible for the observation of an increase in FGF·dp10 at the expense of the FGF·dp10·K_4 ternary complex at high salt.

The extended spectral range at 100 mM salt to include FGF_2·dp10 is shown in Figure 5b. Here, the masses of FGF, K_4, and 2FGF are subtracted from the calculated mass distribution of the complexes in order to compare the sulfation levels of the relevant host dp10 chains. Within the limitations of ESI-MS resolution, the overlapping distributions due to the uncertainty in the number of cationizing agents attached to each polyanionic chain, the higher mean levels of sulfation (S14 and S15) of dp10 within FGF_2·dp10 compared to those within FGF·dp10 complexes (S10−14) were observed, and chains that contain S12−15 appear to bind both FGF and K_4. While chains of low sulfation may bind only one FGF, highly sulfated FGF·dp10 chains appear to be subject to competition between K_4 and FGF for the second binding site. Comparison of the highly sulfated (15S) dp10 species in Figure 5b suggests that FGF preferentially occupies this site. The analysis of dp10 and K_4 complexes at 100 mM indicated that these chains are *not* the preferential targets of K_4 (Figure S1, Supporting Information). Because K_4 binding depends on the condensed layer of counterions, the opposing effects of sulfation density and end effects may explain the absence of a clear effect of the former.

Binding to dp10 by K_4 and FGF differ in several ways. The salt dependence of K_4·dp10 complexation is consistent with binding driven by the release of condensed counterions; on the other hand, FGF binding to dp10 exhibits higher salt resistance and more complex ionic strength dependence consistent with screened electrostatics. While FGF_2·dp10 complexes are formed over a wide range of ionic strength, dp10 can only bind one K_4. Estimates of the size of the FGF binding site on heparin suggest about two disaccharides, similar to the mean protein hydrodynamic radius, that is, 2 nm, consistent with the maximum number of proteins that can bind to native Hp.[60] K_4 (≈2 nm contour length) can then be easily accommodated near the center of dp10, with a distal region of higher effective charge density accessible for FGF. FGF binding is facilitated by high dp10 sulfation, whereas the effect of sulfation levels on K_4 binding can be obscured by the conjoint influence of end effects on the concentration of dp10 condensed counterions.

These observations point out that control of *I* and overall sulfation levels of heparinoids could be used to manipulate the balance between matrix component and growth factor affinity in tissue engineering. The selection of the conditions could be used to influence the rates of morphogen release and also the presence or absence of heparin accompanying the free growth factor. The stability of the FGF·dp10 versus K_4·dp10 complexes at selected conditions will determine which bond will break first in the tissue scaffolds to release FGF, and as a result of this breakage, FGF will be released with or without heparinoid. The use of low ionic strength (<40 mM) during the assembly process should enhance ternary complex formation and higher ionic strength of the environment could lead to the dissociation of the dp10·K_4 bond first; then GF would be released in the heparinoid-bound form during the dissociation process. In addition to addition of salt, increasing the degrees of sulfation definitely promotes capturing a large number of growth factors

dx.doi.org/10.1021/bm401227p | *Biomacromolecules* 2013, 14, 4091−4098

and the formation of ternary complexes. Therefore, heparin chains with higher degrees of sulfation could be used to deliver high concentration of GFs in the tissue environments.

4. Biological Activity of FGF vs FGF·dp10·K_4. We investigated whether the complexation of FGF to dp10 and K4 would alter its bioactivity when compared to FGF alone (Figure 6). HEP3Bs were stimulated with FGF or FGF complex across

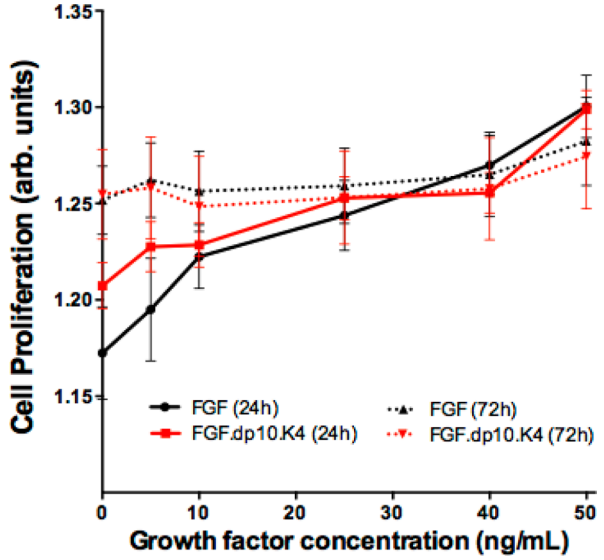

Figure 6. FGF·dp10·K_4 mixture retains biological activity of FGF· HEP3Bs were treated with either FGF (black) or FGF·dp10·K_4 (red), and cell proliferation was quantified at 24 (solid) and 72 h (dashed). No statistical differences were noted when comparing cell proliferation with FGF and the FGF·dp10·K_4, at any time point. Proliferation increases with FGF concentration at 24 h and is maximized at all concentrations at 72 h. In both formats, FGF of 50 ng/mL is statistically higher than the no growth factor condition at 24 h.

concentrations ranging from 0 to 50 ng/mL. We found that binding of dp10 and K4 to FGF does not significantly alter its activity at any of the tested concentrations. As expected, HEP3B proliferation at 24 h increased by approximately 10% with FGF and FGF complex as compared with the control. After 72 h, cell proliferation is maximized, and neither treatment showed any significant difference in proliferation across the concentrations tested here.

CONCLUSIONS

A heparin decamer (dp10) in the presence of tetralysine (K_4) can bind either one or two molecules of acidic fibroblast growth factor (FGF), or FGF and K_4, but cannot bind two molecules of K_4. Using electrospray mass spectrometry (ESI-MS) to investigate the ionic strength effect on the formation of these complexes, we concluded that the formation of K_4·dp10 is driven by the release of condensed counterions. We have previously shown that the concentration of condensed counterions on dp10 is strongly reduced near its chain termini, and therefore propose that K_4 binding is constrained to the central region of dp10. The markedly different ionic strength dependence of FGF binding suggests a different mechanism (based on screened electrostatics), which removes this constraint, so that the growth factor can bind along with K_4 ("ternary complex") or along with a second FGF. ESI-MS characterization of bound dp10 chains in various complexes indicates that FGF binding is enhanced by heparin sulfation, while K_4 binding is relatively indifferent to it due to competing effects. Cell culture studies indicated that complexation of FGF in the form FGF·dp10·K_4 does not significantly change its biological activity. These observations suggest the application of shorter heparin chains as a route to growth factor sequestration and release in tissues matrices could be more effective than the use of heterogeneous native heparin chains. The effects of heparin chain length and mixing ratio of scaffold component (peptide, heparin oligomer, protein) remain to be studied.

ASSOCIATED CONTENT

Supporting Information

The extended ESI mass spectral region of dp10·K_4 complexes in 100 mM, pH 5.5, and dp10 in the K_4-free solution were shown. The mass ranges for dp10 heparinoid species with a different extent of sulfation were indicated with the shaded boxes. This material is available free of charge via the Internet at http://pubs.acs.org.

AUTHOR INFORMATION

Corresponding Author

*E-mail: dubin@chem.umass.edu.

Notes

The authors declare no competing financial interest.

ACKNOWLEDGMENTS

This work was supported by Grants from the National Science Foundation, CHE-0750389 (to I.K.) and CHE-0619039 (to P.D.), for Burcu Baykal Minsky. S.R.P. and T.V.N. were partially supported by a Barry and Afsaneh Siadat Career Development Award. We would like to thank Robert J. Linhardt (RPI, Troy, NY) for providing FGF-1.

REFERENCES

(1) Bishop, J. R.; Schuksz, M.; Esko, J. D. *Nature* **2007**, *446*, 1030−1037.
(2) Esko, J. D.; Selleck, S. B. *Annu. Rev. Biochem.* **2002**, *71*, 435−471.
(3) Sarrazin, S.; Lamanna, W. C.; Esko, J. D. *Cold Spring Harbor Perspect. Biol.* **2011**, *3*, a004952 .
(4) Lander, A. D. *Matrix Biol.* **1998**, *17*, 465−472.
(5) Tae, G.; Scatena, M.; Stayton, P. S.; Hoffman, A. S. *J. Biomater. Sci., Polym. Ed.* **2006**, *17*, 187−197.
(6) Benoit, D. S.; Collins, S. D.; Anseth, K. S. *Adv. Funct. Mater.* **2007**, *17*, 2085−2093.
(7) Benoit, D. S. W.; Anseth, K. S. *Acta Biomater.* **2005**, *1*, 461−470.
(8) Wu, J. M.; Xu, Y. Y.; Li, Z. H.; Yuan, X. Y.; Wang, P. F.; Zhang, X. Z.; Liu, Y. Q.; Guan, J.; Guo, Y.; Li, R. X.; Zhang, H. *J. Mater. Sci.: Mater. Med.* **2010**, *22*, 107−114.
(9) Yamaguchi, N.; Zhang, L.; Chae, B.-S.; Palla, C. S.; Furst, E. M.; Kiick, K. L. *J. Am. Chem. Soc.* **2007**, *129*, 3040−3041.
(10) Yoon, J. J.; Chung, H. J.; Park, T. G. *J. Biomed. Mater. Res., Part A* **2007**, *83A*, 597−605.
(11) Zhang, L.; Furst, E. M.; Kiick, K. L. *J. Controlled Release* **2006**, *114*, 130−142.
(12) Jeon, O.; Powell, C.; Solorio, L. D.; Krebs, M. D.; Alsberg, E. *J. Controlled Release* **2011**, *154*, 258−266.
(13) Seal, B. L.; Panitch, A. *Biomacromolecules* **2003**, *4*, 1572−1582.
(14) Maxwell, D. J.; Hicks, B. C.; Parsons, S.; Sakiyama-Elbert, S. E. *Acta Biomater.* **2005**, *1*, 101−113.
(15) Sakiyama-Elbert, S. E.; Hubbell, J. A. *J. Controlled Release* **2000**, *65*, 389−402.
(16) Wood, M. D.; Sakiyama-Elbert, S. E. *J. Biomed. Mater. Res., Part A* **2008**, *84A*, 300−312.
(17) Manning, G. S. *J. Chem. Phys.* **1969**, *51*, 924−933.
(18) Manning, G. S. *Biophys. Chem.* **1978**, *9*, 65−70.

(19) Lohman, T. M.; deHaseth, P. L.; Record, M. T., Jr. *Biochemistry* **1980**, *19*, 3522−3530.
(20) Mascotti, D. P.; Lohman, T. M. *Proc. Natl. Acad. Sci. U.S.A.* **1990**, *87*, 3142−3146.
(21) Mascotti, D. P.; Lohman, T. M. *Biochemistry* **1995**, *34*, 2908−2915.
(22) Minsky, B. B.; Atmuri, A.; Kaltashov, I. A.; Dubin, P. L. *Biomacromolecules* **2013**, *14*, 1113−1121.
(23) Olson, S. T.; Bjork, I.; Sheffer, R.; Craig, P. A.; Shore, J. D.; Choay, J. *J. Biol. Chem.* **1992**, *267*, 12528−12538.
(24) Thompson, L. D.; Pantoliano, M. W.; Springer, B. A. *Biochemistry* **1994**, *33*, 3831−3840.
(25) Friedrich, U.; Blom, A. M.; Dahlbäck, B.; Villoutreix, B. O. *J. Biol. Chem.* **2001**, *276*, 24122−24128.
(26) Fenley, M. O.; Russo, C.; Manning, G. S. *J. Phys. Chem. B* **2011**, *115*, 9864−9872.
(27) Ashikari-Hada, S.; Habuchi, H.; Kariya, Y.; Itoh, N.; Reddi, A. H.; Kimata, K. *J. Biol. Chem.* **2004**, *279*, 12346−12354.
(28) Ashikari-Hada, S.; Habuchi, H.; Sugaya, N.; Kobayashi, T.; Kimata, K. *Glycobiology* **2009**, *19*, 644−654.
(29) Faham, S.; Hileman, R. E.; Fromm, J. R.; Linhardt, R. J.; Rees, D. C. *Science* **1996**, *271*, 1116−1120.
(30) Zhang, F.; Zhang, Z.; Lin, X.; Beenken, A.; Eliseenkova, A. V.; Mohammadi, M.; Linhardt, R. J. *Biochemistry* **2009**, *48*, 8379−8386.
(31) Jones, L. S.; Yazzie, B.; Middaugh, C. R. *Mol. Cell. Proteomics* **2004**, *3*, 746−769.
(32) Kayitmazer, A. B.; Quinn, B.; Kimura, K.; Ryan, G. L.; Tate, A. J.; Pink, D. A.; Dubin, P. L. *Biomacromolecules* **2010**, *11*, 3325−3331.
(33) Seyrek, E.; Dubin, P. L.; Henriksen, J. *Biopolymers* **2007**, *86*, 249−259.
(34) Seyrek, E.; Dubin, P. L.; Tribet, C.; Gamble, E. A. *Biomacromolecules* **2003**, *4*, 273−282.
(35) Seyrek, E.; Dubin, P. *Adv. Colloid Interface Sci.* **2010**, *158*, 119−129.
(36) Jemth, P.; Kreuger, J.; Kusche-Gullberg, M.; Sturiale, L.; Gimenez-Gallego, G.; Lindahl, U. *J. Biol. Chem.* **2002**, *277*, 30567−30573.
(37) Kreuger, J.; Jemth, P.; Sanders-Lindberg, E.; Eliahu, L.; Ron, D.; Basilico, C.; Salmivirta, M.; Lindahl, U. *Biochem. J.* **2005**, *389*, 145−150.
(38) Catlow, K. R.; Deakin, J. A.; Wei, Z.; Delehedde, M.; Fernig, D. G.; Gherardi, E.; Gallagher, J. T.; Pavao, M. S.; Lyon, M. *J. Biol. Chem.* **2008**, *283*, 5235−5248.
(39) Jastrebova, N.; Vanwildemeersch, M.; Lindahl, U.; Spillmann, D. *J. Biol. Chem.* **2010**, *285*, 26842−26851.
(40) Jastrebova, N.; Vanwildemeersch, M.; Rapraeger, A. C.; Gimenez-Gallego, G.; Lindahl, U.; Spillmann, D. *J. Biol. Chem.* **2006**, *281*, 26884−26892.
(41) Chen, K.; Xu, Y.; Rana, S.; Miranda, O. R.; Dubin, P. L.; Rotello, V. M.; Sun, L.; Guo, X. *Biomacromolecules* **2011**, *12*, 2552−2561.
(42) Xu, Y.; Engel, Y.; Yan, Y.; Chen, K.; Moyano, D. F.; Dubin, P. L.; Rotello, V. M. *J. Mater. Chem., Part B* **2013**, *1*, 5230−5234.
(43) Kayitmazer, A. B.; Seeman, D.; Minsky, B. B.; Dubin, P. L.; Xu, Y. *Soft Matter* **2013**, *9*, 2553−2583.
(44) Seyrek, E.; Dubin, P. L.; Henriksen, J. *Biopolymers* **2007**, *86*, 249−259.
(45) Schreiber, G.; Haran, G.; Zhou, H. X. *Chem. Rev.* **2009**, *109*, 839−860.
(46) Perez Sanchez, H.; Tatarenko, K.; Nigen, M.; Pavlov, G.; Imberty, A.; Lortat-Jacob, H.; Garcia de la Torre, J.; Ebel, C. *Biochemistry* **2006**, *45*, 13227−13238.
(47) Manning, G. S. *Macromolecules* **2008**, *41*, 6217−6227.
(48) Faham, S.; Linhardt, R. J.; Rees, D. C. *Curr. Opin. Struct. Biol.* **1998**, *8*, 578−586.
(49) Johnson, D. J.; Li, W.; Adams, T. E.; Huntington, J. A. *EMBO J.* **2006**, *25*, 2029−2037.
(50) Abzalimov, R. R.; Dubin, P. L.; Kaltashov, I. A. *Anal. Chem.* **2007**, *79*, 6055−6063.
(51) Rosu, F.; Gabelica, V.; Poncelet, H.; De Pauw, E. *Nucleic Acids Res.* **2010**, *38*, 5217−5225.
(52) Park, A. Y.; Robinson, C. V. *Crit. Rev. Biochem. Mol. Biol.* **2011**, *46*, 152−164.
(53) Kim, J.; Blaber, S. I.; Blaber, M. *Protein Sci.* **2002**, *11*, 459−466.
(54) Rocchia, W.; Alexov, E.; Honig, B. *J. Phys. Chem. B* **2001**, *105*, 6507−6514.
(55) Rocchia, W.; Sridharan, S.; Nicholls, A.; Alexov, E.; Chiabrera, A.; Honig, B. *J. Comput. Chem.* **2002**, *23*, 128−137.
(56) Tanford, C.; Kirkwood, J. G. *J. Am. Chem. Soc.* **1957**, *79*, 5333−5339.
(57) Record, M. T., Jr.; Lohman, M. L.; De Haseth, P. *J. Mol. Biol.* **1976**, *107*, 145−158.
(58) Grymonpre, K. R.; Staggemeier, B. A.; Dubin, P. L.; Mattison, K. W. *Biomacromolecules* **2001**, *2*, 422−429.
(59) Vijayakumar, M.; Wong, K. Y.; Schreiber, G.; Fersht, A. R.; Szabo, A.; Zhou, H. X. *J. Mol. Biol.* **1998**, *278*, 1015−1024.
(60) Mach, H.; Volkin, D. B.; Burke, C. J.; Middaugh, C. R.; Linhardt, R. J.; Fromm, J. R.; Loganathan, D.; Mattsson, L. *Biochemistry* **1993**, *32*, 5480−5489.
(61) Muthukumar, M. *J. Chem. Phys.* **1987**, *86*, 7230−7235.
(62) Vongoeler, F.; Muthukumar, M. *J. Chem. Phys.* **1994**, *100*, 7796−7803.
(63) Cooper, C. L.; Goulding, A.; Kayitmazer, A. B.; Ulrich, S.; Stoll, S.; Turksen, S.; Yusa, S.; Kumar, A.; Dubin, P. L. *Biomacromolecules* **2006**, *7*, 1025−1035.
(64) Henriksen, J.; Ringborg, L. H.; Roepstorrf, P. *J. Mass Spectom.* **2004**, *39*, 1305−1312.